

PHYSICAL REVIEW B

CONDENSED MATTER

THIRD SERIES, VOLUME 39, NUMBER 16 PART B

1 JUNE 1989

Random-walk simulation of diffusion-controlled processes among static traps

Sang Bub Lee, In Chan Kim, and C. A. Miller

Department of Mechanical and Aerospace Engineering, North Carolina State University, Raleigh, North Carolina 27695-7910

S. Torquato*

*Department of Mechanical and Aerospace Engineering and Department of Chemical Engineering,
North Carolina State University, Raleigh, North Carolina 27695-7910*

(Received 7 November 1988)

We present computer-simulation results for the trapping rate (rate constant) k associated with diffusion-controlled reactions among identical, static spherical traps distributed with an arbitrary degree of impenetrability using a Pearson random-walk algorithm. We specifically consider the penetrable-concentric-shell model in which each trap of diameter σ is composed of a mutually impenetrable core of diameter $\lambda\sigma$, encompassed by a perfectly penetrable shell of thickness $(1-\lambda)\sigma/2$: $\lambda=0$ corresponding to randomly centered or "fully penetrable" traps and $\lambda=1$ corresponding to totally impenetrable traps. Trapping rates are calculated accurately from the random-walk algorithm at the extreme limits of λ ($\lambda=0$ and 1) and at an intermediate value ($\lambda=0.8$), for a wide range of trap densities. Our simulation procedure has a relatively fast execution time. It is found that k increases with increasing impenetrability at fixed trap concentration. These "exact" data are compared with previous theories for the trapping rate. Although a good approximate theory exists for the fully-penetrable-trap case, there are no currently available theories that can provide good estimates of the trapping rate for a moderate to high density of traps with nonzero hard cores ($\lambda > 0$).

I. INTRODUCTION

Diffusion-controlled reactions play an important role in a host of phenomena, including migration of atoms and defects in solids, heterogeneous catalysis, combustion of liquid droplets, polymer chain growth kinetics, colloid or crystal growth, precipitation, and fluorescence quenching. A diffusion-controlled reaction is one in which the time for two bodies to diffuse in the same neighborhood is the rate-limiting step, the reaction time being negligible in comparison. Often one of the reaction partners is large and may be regarded as static. Thus one considers media composed of static traps (sinks) distributed throughout a region containing reactive particles. The reactant diffuses in the trap-free region but is instantly absorbed on contact with any trap. At steady state (the subject of this article), the rate of production of the diffusing species is exactly compensated by its removal by the traps. At sufficiently low trap densities, such that interactions between traps can be neglected, Smoluchowski¹ derived an expression for the trapping rate (rate constant) k for spherical traps. For arbitrary trap density, there will be a competition between traps and the trapping rate k will depend upon the concentration of traps.²

This paper reports computer-simulation results for the

steady-state trapping rate k of a medium containing a random distribution of identical, static, perfectly absorbing, spherical traps of radius R (which generally may overlap one another in varying degrees) for arbitrary trap volume fraction ϕ_2 . This is accomplished by considering a Pearson random walk in which the step size a is fixed and successive directions are random and uncorrelated.³ The trapping rate is simply the inverse of the average time taken for the random walkers to get trapped, \bar{t} . Now if \bar{n} denotes the mean number of steps taken by the random walkers and $\bar{n} \gg 1$, then the random walk becomes simple Brownian motion and we have

$$\bar{t} = \frac{\bar{n}a^2}{6D}, \quad (1)$$

where D is the diffusion coefficient. For a dilute concentration of spherical traps at steady state, Smoluchowski¹ found

$$k_s = \frac{3D\phi_2}{R^2}, \quad (2)$$

and hence combination of Eq. (2) with the preceding results gives, for arbitrary ϕ_2 , that

$$\frac{k}{k_s} = \frac{2}{\bar{n}\phi_2} \left[\frac{R}{a} \right]^2. \quad (3)$$

By measuring \bar{n} for a given ϕ_2 , one may compute the trapping rate k using Eq. (3). Now, since \bar{n} must be large, then the step size a must be small compared to R in our simulations. Accordingly, we compute k/k_s for fixed ϕ_2 by varying the step size a and then extrapolating to the $a/R \rightarrow 0$ limit. Extrapolation is especially necessary at high trap volume fraction ϕ_2 .

Another way of computing the trapping rate is to calculate the mean-square displacement $r^2 = \bar{n}a^2$ for the random walkers before trapping,⁴ i.e., employ the relation

$$\frac{k}{k_s} = \frac{2R^2}{\phi_2 r^2}. \quad (4)$$

As a consistency check, we also compute the right-hand side of Eq. (4) for various values of a and extrapolate to the $a/R \rightarrow 0$ limit.

We specifically consider a distribution of spherical traps in the penetrable-concentric-shell (PCS) (Ref. 5) model. In the PCS model (depicted in Fig. 1), each sphere of radius R is composed of an impenetrable core of radius λR , encompassed by a perfectly penetrable concentric shell of thickness $(1-\lambda)R$, $0 \leq \lambda \leq 1$. The extreme limits $\lambda=0$ and $\lambda=1$ correspond, respectively, to the cases of "fully penetrable" (i.e., randomly centered) and "totally impenetrable" spheres. For $\lambda > 0$ (i.e., for finite-sized hard cores), the impenetrability condition alone does not uniquely determine the distribution. One may assume an equilibrium distribution⁶ or some nonequilibrium ensemble, such as random sequential addition (RSA).⁷ In this study, we shall compute k for an equilibrium distribution of spheres in the PCS model at $\lambda=0, 0.8$, and 1 for a wide range of trap volume functions.

The PCS model is versatile in that it enables one to vary the degree of the connectedness of the particle phase by varying the degree of impenetrability λ . For example, for equilibrium ensembles of fully penetrable ($\lambda=0$) and totally impenetrable ($\lambda=1$) spheres, the particle phase percolates (i.e., a sample-spanning cluster appears) at a

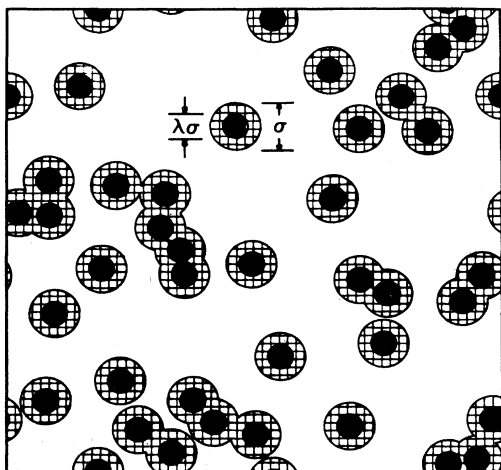


FIG. 1. A computer-generated realization of a distribution of disks of radius $R = \sigma/2$ in the PCS model (Ref. 5). The disks have an impenetrable core of diameter $\lambda\sigma$ indicated by the smaller, black circular region. Here $\lambda=0.5$ and ϕ_2 is about 0.3.

sphere volume fraction ϕ_2 of about 0.3 (Ref. 8) and 0.63 (Ref. 9), respectively. (A distribution of fully penetrable spheres is a bicontinuous medium for $0.3 \leq \phi_2 \leq 0.97$, where $\phi_2=0.97$ corresponds to the point at which the matrix phase fails to percolate.¹⁰)

In a series of ground-breaking papers, Richards¹¹⁻¹³ developed a theory to study the rate of diffusion-controlled reactions among static, spherical traps. His theory centered on obtaining the survival probability $S(t)$ which gives the probability that a random walker which was not at a trap site at time $t=0$ has still not encountered a trap at time t . Clearly, the rate constant is related to the survival probability by the relation

$$k^{-1} = \int S(t) dt. \quad (5)$$

Richards obtained k for two different distributions of spherical traps: (1) fully penetrable spheres¹² and (2) totally impenetrable spheres.¹³ In order to test his theory, Richards carried out Monte Carlo computer simulations using a lattice random-walk algorithm [in conjunction with Eq. (1)] for fully penetrable spheres¹² and totally impenetrable spheres distributed according to a random sequential addition process.¹³ Since Richards's main interest was to confirm his theory, his simulation study was not intended to be comprehensive in nature.

Our simulations differ from Richards's simulations^{12,13} in several ways. First, he utilizes a lattice random-walk algorithm, whereas we employ a "continuum" random-walk technique, i.e., the Pearson random walk described above. As lattice random walks are restricted to move only along the coordinate axes directions, one would expect raw data to contain some error due to the lattice effects. (Extrapolating the data to the $a/R \rightarrow 0$ limit, of course, essentially eliminates lattice effects.) Most of Richards's data^{12,13} were obtained for relatively large step sizes (up to $R/a=6$) and in most cases were determined without extrapolation. Our Pearson random walks are performed for a wide range of step sizes (from $R/a=4$ to $R/a=60$, depending upon the volume fraction) and the resulting data are always extrapolated to the $a/R \rightarrow 0$ limit. Second, we examine the more general PCS model, of which the fully-penetrable-sphere limit ($\lambda=0$) is a special case. Although Richards studied totally impenetrable sinks, this distribution was generated using an RSA process which is known to be generally quite different than the equilibrium distribution employed in the present investigation.⁷ For example, the radial distribution function (at moderate to high densities) and the close-packing volume fractions are known to be different for these two distributions.¹⁴ RSA configurations are generated by sequentially adding particles to the unit cell. The process continues until there is no accessible space for additional particles. The final state is known as the "jamming limit" which is considerably smaller than the random close-packing limit associated with equilibrium distributions.¹⁴ The maximum volume fraction which Richards¹³ could obtain using RSA was $\phi_2 \approx 0.41$, which is much less than the accepted value $\phi_2 \approx 0.63 \pm 0.01$ corresponding to random close packing.⁹ For $\lambda=1$, we report the trapping rate k up to $\phi_2=0.6$. We also examine the intermediate case $\lambda=0.8$. Third, we compute k at

fixed λ for a large number of volume fractions. In his study of fully penetrable spheres,¹² for example, Richards reported k for only a single volume fraction of traps. Fourth, we employ a GRID method¹⁵ to speed up the time required to test if a walker has been trapped.

In Sec. II, we describe our simulation procedure. In Sec. III, we present and discuss our results for the trapping rate in the PCS model. Our results are compared to Richards's theory^{12,13} and Torquato's¹⁶ calculations of rigorous lower bounds on the trapping rate for the extreme cases of fully penetrable and totally impenetrable spheres. In Sec. IV, we make concluding remarks.

II. SIMULATION PROCEDURE

Obtaining the trapping rate from our computer simulations is a two-step process. First, one must generate realizations of the random medium which, in this study, are distributions of spherical traps at volume fraction ϕ_2 in the PCS model. Second, employing a Pearson random-walk algorithm, we determine the trapping rate per realization and then average over a sufficiently large number of realizations to obtain k .

Consider each sphere to have a radius R and an inner impenetrable core of radius λR . Because of interparticle overlap one cannot fix the sphere volume fraction *a priori* in a simulation.¹⁵ One can fix the reduced number density $\eta = \rho 4\pi R^3/3$ (where ρ is the sphere number density) and then determine the volume fraction ϕ_2 .¹⁵ For the extreme cases $\lambda=0$ and 1, the relations between ϕ_2 and η are simple analytical expressions: $\phi_2 = \eta$ for $\lambda=1$ and $\phi_2 = 1 - \exp(-\eta)$ for $\lambda=0$. For intermediate λ and arbitrary η , the theoretical determination of ϕ_2 is nontrivial [although the inequality $\phi_2(\lambda=1) > \phi_2(\lambda)$ for $\lambda < 1$ and fixed η is known to apply generally]. From a simulation standpoint, the problem becomes nontrivial if the degree of overlap is nonzero, i.e., $0 \leq \lambda < 1$. Lee and Torquato¹⁵ recently computed ϕ_2 as a function of η for fixed λ in the two- and three-dimensional PCS model using computer-simulation methods. Certain aspects of the Lee-Torquato study shall be incorporated in the present investigation. It should be mentioned that the specific surface s (interfacial surface area) for totally impenetrable spheres is always greater than s for $\lambda < 1$ at fixed ϕ_2 . Accordingly, the trapping rate is expected to increase as λ increases.

In order to generate equilibrium realizations of spheres for fixed λ and reduced number density η , we employ a conventional Metropolis algorithm.¹⁷ Particles are initially placed, with no hard-core overlaps, on the lattice sites of a body-centered cubic array in a cubical cell of volume L^D . The cell is surrounded by periodic images of itself. Each particle is then moved by a small distance to a new position which was accepted or rejected according to whether or not inner hard cores overlapped. This process is repeated many times until equilibrium is achieved.

Our system contains 490 particles in a given cell, and each particle is moved 200 times before sampling for equilibrium realizations. (Compared to previous simulations of related transport properties, a 490-particle system is a very large system and was found to be sufficiently large to ignore finite-size errors.) Trap distributions were sampled at intervals of 10–20 moves per particle. In or-

der to ensure that equilibrium is achieved, we determine the pressure as a function of η for a system of particles having diameter $2\lambda R$. The pressures so obtained were in very good agreement with the accurate Carnahan-Starling equation.¹⁸

The next step involves carrying out a large number of Pearson random walks per realization in order to compute the mean number of steps \bar{n} , Eq. (3), and the mean-square trapping displacement \bar{r}^2 , Eq. (4), for fixed η and λ . Random walkers are initially placed at randomly chosen points in the trap-free region. The walkers then undergo a Pearson random walk until they encounter the trapping region. If \mathbf{x} represents the position vector of the random walker and \mathbf{s}_i denotes the position of the center of the i th neighboring particle, then the walker is considered to be trapped if

$$|\mathbf{x} - \mathbf{s}_i| \leq R \text{ for } i = 1, 2, \dots, m, \quad (6)$$

where m is the number of neighboring particles. Searching for neighboring particles must be carried out efficiently. One can use a so-called "cell-list" method,¹⁹ i.e., divide the system volume into cubical cells, each with sides of length $2R$. One then checks for particles in the nearest- and next-nearest cells. We found, however, that this method required an enormous amount of computing time, most of which was spent to check trapping for each step of the random walk.

In order to significantly reduce computing time, we employ the so-called GRID method employed previously by Lee and Torquato¹⁵ to measure the porosity of random media composed of D -dimensional distributions of spheres in the PCS model. Spherical traps are placed in a unit cell which is tessellated into cubical pixels with a resolution of $80 \times 80 \times 80$ (i.e., about 10 pixels per diameter). We then determine whether each pixel lies entirely in the trap or trap-free region or if it contains an edge of the two-phase interface. Initially pixels are "unpainted" (an integer 0 is assigned). If a pixel lies entirely in the particle phase, it is painted (an integer 1 is assigned). If it contains an edge of the two-phase interface, the pixel is assigned a particle identification number which ranges from 2 to $N+1$, where N is the total number of particles. Pixels containing more than one particle edge are stored in a separate table. Associated with each column of the table are the particle identification numbers, and each pixel is denoted by the negative of the corresponding column numbers. Once the pixel image of the trap distribution is completed, trapping of the random walkers can readily be determined. Testing Eq. (6) is necessary *only* when the random walker chooses the next step to be in a pixel which contains the two-phase interface. Particles that need to be checked for trapping are identified immediately from the integer assigned on the pixel array. Note that the number of such particles is also greatly reduced relative to the cell-list method.

When a random walker is considered trapped, the walk is terminated and the time and distance traveled by the walker are stored. For each step size a , reduced density η , impenetrability index λ , and realization, we carry out 1000 random walks and average over the walks to obtain \bar{n} and \bar{r}^2 . This process is repeated for four smaller step

TABLE I. Range of scaled step sizes for each value of the reduced density $\eta=4\rho\pi R^3/3$ and impenetrability parameter: (i) $R/a=4, 5, 7, 10,$ and 15 ; (ii) $R/a=5, 7, 10, 15,$ and 25 ; (iii) $R/a=7, 10, 15, 25,$ and 40 ; (iv) $b/a=10, 15, 25, 40,$ and 60 . Here a and R are the step size and particle radius, respectively.

| η | $\lambda=1$ | $\lambda=0$ | $\lambda=0.8$ |
|--------|-------------|-------------|---------------|
| 0.10 | i | | i |
| 0.20 | ii | ii | ii |
| 0.25 | ii | | |
| 0.30 | ii | ii | ii |
| 0.35 | ii | | |
| 0.40 | ii | ii | ii |
| 0.45 | ii | | |
| 0.50 | iii | ii | ii |
| 0.55 | iii | | |
| 0.60 | iv | ii | ii |
| 0.70 | | | ii |
| 0.80 | | ii | ii |
| 0.90 | | | iii |
| 1.00 | | ii | iii |
| 1.20 | | ii | |
| 1.40 | | iii | |
| 1.60 | | iii | |
| 1.80 | | iii | |
| 2.00 | | iii | |
| 2.30 | | iv | |

sizes. Thus, the total number of step sizes we consider is five. Results are then averaged over 100 realizations for each value of η and λ and, for selected η and λ , are averaged over 250 realizations. The step sizes used in our simulations are listed in Table I.

III. RESULTS AND DISCUSSIONS

Our simulation results for k/k_s were found to increase linearly with decreasing step size. The final results reported here were obtained by extrapolating to the $a/R \rightarrow 0$ limit. In a recent theoretical study, Ziff²⁰ showed that the trapping rate for a random walker in a medium containing a single spherical trap is indeed linear in the step size. Interestingly, we find the same trend for many traps.

The trapping rates obtained from Eqs. (3) and (4) were basically very close to each other, as expected, and the difference ranged between 0.06 and 0.6% for all models of trap particles. The simulation results reported here were determined from Eq. (3). Results for the impenetrability parameter $\lambda=0, 0.8,$ and 1 are summarized in Tables II, III, and IV, respectively. The data represent averages over 100 realizations. Values of \bar{n} from realization to realization changed very little. For selected values of η and λ , we averaged over an additional 150 realizations for a total of 250 realizations. In these instances, we first obtained "batch" averages and then averaged over the number of batch runs; each batch run was an average over 50 realizations. The largest deviations between pairs of batch runs were very small, varying between 0.02 and 1.2%. The standard deviations were also small, e.g., at $\eta=0.8$ for $\lambda=0$, the scaled rate constant k/k_s was found to be 4.752 ± 0.048 ; and at $\eta=0.2$ and

TABLE II. The scaled trapping rate k/k_s obtained from Eq. (3) for fully penetrable traps ($\lambda=0$) in the limit $a/R \rightarrow 0$. Here η and ϕ_2 are, respectively, the reduced density and the trap volume fraction.

| η | ϕ_2 | k/k_s |
|--------|----------|---------|
| 0.2 | 0.181 27 | 2.017 |
| 0.3 | 0.259 18 | 2.476 |
| 0.4 | 0.329 68 | 2.837 |
| 0.5 | 0.393 47 | 3.301 |
| 0.6 | 0.451 19 | 3.735 |
| 0.8 | 0.550 67 | 4.739 |
| 1.0 | 0.632 12 | 5.834 |
| 1.2 | 0.698 81 | 6.822 |
| 1.4 | 0.753 40 | 8.199 |
| 1.6 | 0.798 10 | 9.765 |
| 1.8 | 0.834 70 | 11.273 |
| 2.0 | 0.864 66 | 13.03 |
| 2.3 | 0.899 74 | 16.15 |

0.5 for $\lambda=1$, $k/k_s=3.219 \pm 0.013$ and $k/k_s=13.89 \pm 0.19$, respectively. Averages over two batch runs (100 realizations) are seen to be within the relatively small error bars associated with averages over five batch runs (250 realizations), thus justifying the less-computer-intensive calculations of averaging over 100 realizations.

Before discussing these results in more detail, we would like to comment on the relatively small amount of computing time required to obtain k/k_s with the high accuracy just described. Recall that each value of k/k_s reported in Tables II–IV was obtained by considering 1000 random walks per realization (consisting of 490 particles) for five different step sizes, extrapolating to the $a/R \rightarrow 0$ limit, and finally by averaging the extrapolated values over 100 realizations. Generally speaking, for fixed η , the computing time increased with decreasing λ ; the cases $\lambda=0$ required between 4.5 and 9 CPU hours (on a VAX 3200) and the instances $\lambda=1$ required between 1.5 and 6 CPU hours. Considering that our comprehensive random-walk simulations employ an order of magni-

TABLE III. The scaled trapping rate k/k_s obtained from Eq. (3) for $\lambda=0.8$ in the PCS model (Ref. 5) in the limit $a/R \rightarrow 0$. Here η and ϕ_2 are, respectively, the reduced density and the trap volume fraction. The relation between η and ϕ_2 is obtained from Ref. 15.

| η | ϕ_2 | k/k_s |
|--------|----------|---------|
| 0.1 | 0.090 61 | 1.945 |
| 0.2 | 0.198 44 | 2.592 |
| 0.3 | 0.295 83 | 3.560 |
| 0.4 | 0.391 51 | 4.837 |
| 0.5 | 0.484 63 | 6.627 |
| 0.6 | 0.575 22 | 8.970 |
| 0.7 | 0.659 56 | 12.47 |
| 0.8 | 0.737 55 | 17.27 |
| 0.9 | 0.812 80 | 26.66 |
| 1.0 | 0.883 95 | 40.53 |

TABLE IV. The scaled trapping rate k/k_s , obtained from Eq. (3) for $\lambda=1$ in the limit $a/R \rightarrow 0$. Here η and ϕ_2 are, respectively, the reduced density and the trap volume fraction.

| η | ϕ_2 | k/k_s |
|--------|----------|---------|
| 0.10 | 0.10 | 2.032 |
| 0.20 | 0.20 | 3.230 |
| 0.25 | 0.25 | 3.949 |
| 0.30 | 0.30 | 4.964 |
| 0.35 | 0.35 | 6.107 |
| 0.40 | 0.40 | 7.677 |
| 0.45 | 0.45 | 9.899 |
| 0.50 | 0.50 | 13.74 |
| 0.55 | 0.55 | 18.25 |
| 0.60 | 0.60 | 23.67 |

tude more particles than other simulation techniques used to compute related transport properties of random media,²¹ our algorithm has a relatively fast execution time.²²

Results for k/k_s for fully penetrable traps are plotted in Fig. 2 and compared with the rigorous interfacial-surface lower bound^{23,24} computed by Torquato^{16,25} and also with analytical calculation by Richards.¹² Monte Carlo data lie above the rigorous lower bound and are slightly below Richards's theoretical expression given by

$$\frac{k}{k_s} = \frac{\eta}{\phi_2 [1 - \sqrt{\pi} \eta e^{y^2} \operatorname{erfc}(y)]}, \quad (7)$$

where $y = (3\eta/\pi)^{1/2}$. The latter expression, which was claimed to be an upper bound, provides a good estimate of the trapping rate for a wide range of volume fractions:

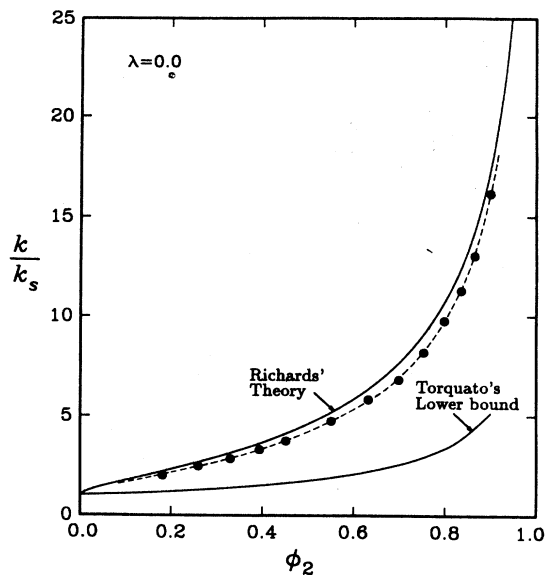


FIG. 2. Trapping rates for fully penetrable spherical traps ($\lambda=0$) as a function of trap volume fraction ϕ_2 . The dashed line is a spline fit of the simulation data (solid circles). Included in the plot is Richards's theory (Ref. 12), and the interfacial-surface lower bound computed by Torquato (Ref. 16).

the greatest deviations occurring at relatively high volume fractions ($0.6 < \phi_2 < 0.8$). Note that for low trap concentrations, Eq. (7) yields

$$\frac{k}{k_s} = 1 + \sqrt{3}\eta^{1/2} + \dots, \quad (8)$$

where the ellipsis represents higher-order terms, which shows the nonanalytic dependence on density first described by Felderhof and Deutch.² The latter authors actually studied *totally impenetrable* traps and found

$$\frac{k}{k_s} = 1 + \sqrt{3}\phi_2^{1/2} + \dots. \quad (9)$$

Recall that $\phi_2 = \eta$ only for $\lambda=1$; for $\lambda=0$, $\phi_2 = 1 - \exp(-\eta)$. To lowest order in η , however, $\phi_2 = \eta$, and hence relations (8) and (9) are equivalent. As noted in the Introduction, Richards¹² computed k for this model for the single volume fraction $\phi_2 = \frac{1}{3}$ and a single step size $R/a = 5$ using a lattice random-walk simulation technique. Our corresponding result is considerably higher than his result. In a subsequent paper, Richards and Torquato²⁶ presented simulation results for this volume fraction and for $\phi_2 = 0.9$ by extrapolating results for various step sizes to the $R/a \rightarrow 0$ limit. These two data are in good agreement with our results.

Results for k/k_s for impenetrable spherical traps are plotted in Fig. 3, and compared with the interfacial-surface lower bound^{23,24} by Torquato¹⁶ and with the theoretical prediction of Richards.¹³ Our simulation data are above the rigorous lower bound for the entire range of ϕ_2 studied here. For $\phi_2 < 0.3$, Richards's prediction overestimates the trapping rate. However, for $\phi_2 > 0.3$, the data sharply increase and rise above Richards's theory. In fact, his result violates the rigorous lower bound for $\phi_2 \approx 0.5$. There are two possible reasons why

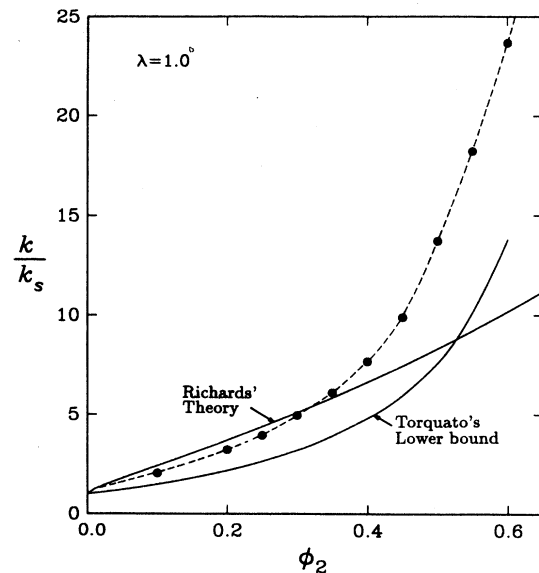


FIG. 3. As in Fig. 2 for totally impenetrable spherical traps ($\lambda=1$). Included in the plot is Richards's theory (Ref. 12), and the interfacial-surface lower bound computed by Torquato (Ref. 16).

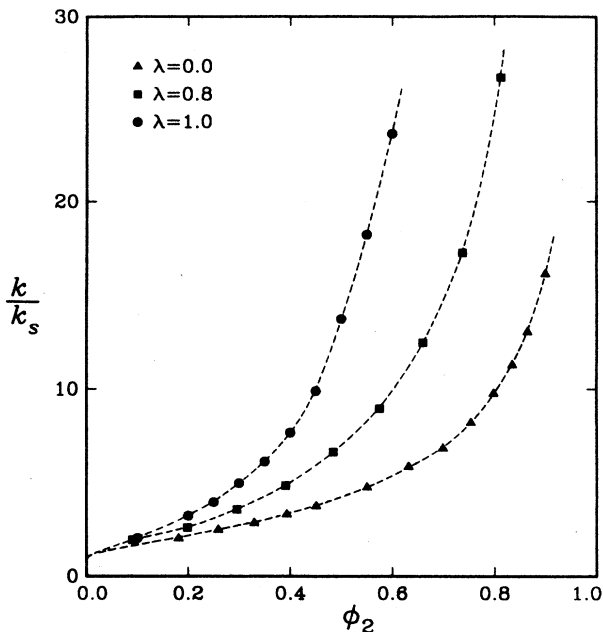


FIG. 4. Trapping rates for spherical traps in the penetrable-concentric-shell model for $\lambda=0, 0.8$, and 1. Dashed lines are spline fits of the simulation data (solid symbols).

Richards's theory breaks down at high trap concentrations. First, he makes use of a second cumulant approximation to obtain his expression. One can in fact show that going to the next (third) cumulant has the effect of increasing k relative to Richards's result. Second, he employs a step function for the radial distribution function $g(r)$, i.e., Richards employs $g(r)=0$ for $r < 2R$, and unity otherwise. This radial distribution function is exact in the zero-density limit. For higher densities, however, $g(r)$ is known to oscillate about its long-range value of unity in a complex fashion. It can further be shown that use of the full density-dependent $g(r)$ tends to decrease k in the second cumulant approximation, so that the agreement obtained by Richards for $\phi_2 < 0.3$ may be somewhat fortuitous: although for very dilute conditions, Richards's expression agrees with relation (9). [For totally impenetrable traps, we carried out simulations for $\phi_2 \leq 0.05$ (not shown) and found good agreement with Eq. (9).] Observe that we report data for $\lambda=1$ up to $\phi_2=0.6$; a value which is near the random-close-packing limit of $\phi_2=0.63 \pm 0.01$ (Ref. 9). Finally, we note that the corrected effective-medium theory of Cukier and Freed²⁷ significantly overestimates the trapping rate at high volume fractions.

In Fig. 4 we plot our simulation results for the scaled

trapping rate at the intermediate value of the impenetrability parameter $\lambda=0.8$. For purposes of comparison we have included in the figure the previously discussed results for $\lambda=0$ and 1. For $\lambda=0.8$, we determined the relationship between the reduced density η and the sphere volume fraction ϕ_2 from the simulation results of Ref. 15. The rate constant for $\lambda=0.8$ lies roughly between the trapping rates for the extreme values of λ . As $\phi_2 \rightarrow 0$, trap interactions become negligible and the data for all three cases approach, as expected. For arbitrary and fixed ϕ_2 , the trapping rate increases with increasing λ . This is physically reasonable since the surface area available for reaction increases as λ increases for fixed ϕ_2 (see discussion at the beginning of Sec. II).

IV. CONCLUSIONS

We have devised an efficient continuum random-walk algorithm which enables us to compute the rate constant for diffusion-controlled reactions among static, perfectly absorbing traps. In particular, we consider an equilibrium ensemble of spherical traps in the PCS model and find that the trapping rate, at fixed trap density, increases with an increase in the impenetrability parameter λ . Our random-walk simulation technique combined with the GRID method (to test trapping) is seen to have a relatively fast execution time. Although Richards's theory provides good estimates of k for fully penetrable traps, there are presently no available theories which accurately predict k for traps with nonzero hard cores at moderate to high densities. In a future study, it would be of interest to employ our simulation technique to examine the effect of spatial dimension on k . It is recommended that similar random-walk algorithms (with some modifications) be employed to compute related transport properties of continuum models of disordered media (e.g., effective electrical conductivity, dielectric constant, etc.).

Note added in proof. We recently learned of a study by L. H. Zheng and Y. C. Chiew [J. Chem. Phys. **90**, 322 (1989)] that estimates k by simulating the Brownian motion of a diffusing particle as we do but with a different algorithm. Their study is less comprehensive than the present one in that they only consider the extreme limits of the PCS model and employ 50–200 particles (as opposed to 490 particles in our simulations). Nonetheless, on the scale of our figures, mutual results are in good agreement.

ACKNOWLEDGMENTS

The authors gratefully acknowledge the support of the Office of Basic Energy Sciences, U.S. Department of Energy, under Grant No. DE-FG05-86ER13482.

* Author to whom all correspondence should be addressed.

¹M. V. Smoluchowski, Phys. Z. **17**, 557 (1916).

²B. U. Felderhof and J. M. Deutch, J. Chem. Phys. **64**, 4551 (1976).

³S. Chandrasekhar, Rev. Mod. Phys. **15**, 1 (1943).

⁴For random walks of various lengths, the mean-square end-to-end distance is defined as $r^2 = \sum_{\text{all walks}} r^2 / \sum_{\text{all walks}} 1$. Grouping out walks having the same number of steps and using the well-known relation $\langle r^2 \rangle = na^2$ for (fixed) n -step walks, one

- can write $\overline{r^2} = \sum_{n=1}^{n_{\max}} \gamma_n n a^2 / \sum_{n=1} \gamma_n$. Here γ_n is the number of n -step walks and n_{\max} is the maximum number of steps a random walker can take. Thus the exact relation $\overline{r^2} = \bar{n} a^2$ follows immediately.
- ⁵S. Torquato, *J. Chem. Phys.* **81**, 5079 (1984); **83**, 4776 (1985); **84**, 6345 (1986).
- ⁶J. P. Hansen and I. R. McDonald, *Theory of Simple Liquids* (Academic, New York, 1976).
- ⁷B. Widom, *J. Chem. Phys.* **44**, 3888 (1966).
- ⁸See, for example, S. W. Haan and R. Zwanzig, *J. Phys. A* **10**, 1547 (1977), and references therein.
- ⁹See, for example, J. G. Berryman, *Phys. Rev. A* **27**, 1053 (1983), and references therein.
- ¹⁰J. Kertész, *J. Phys. Lett. (Paris)* **42**, L393 (1981); W. T. Elam, A. R. Kerstein, and J. J. Rehr, *Phys. Rev. Lett.* **52**, 1516 (1984).
- ¹¹P. M. Richards, *Phys. Rev. Lett.* **56**, 1838 (1986).
- ¹²P. M. Richards, *J. Chem. Phys.* **85**, 3520 (1986).
- ¹³P. M. Richards, *Phys. Rev. B* **35**, 248 (1987).
- ¹⁴J. Feder, *J. Theor. Biol.* **87**, 237 (1980); P. A. Smith and S. Torquato, *J. Comput. Phys.* **76**, 176 (1988).
- ¹⁵S. B. Lee and S. Torquato, *J. Chem. Phys.* **89**, 3258 (1988).
- ¹⁶S. Torquato, *J. Chem. Phys.* **85**, 7178 (1986). In order to convert results for the rate constant in this study to the definition of the rate constant in the present paper, one must multiply the latter results by $(1 - \phi_2)^2$. See Ref. 26 for an explanation of the relationships between the various definitions of the rate constant that have arisen in the literature.
- ¹⁷N. Metropolis, A. W. Rosenbluth, M. N. Rosenbluth, A. N. Teller, and E. Teller, *J. Chem. Phys.* **21**, 1087 (1953); see also W. W. Woods, in *Physics of Simple Liquids*, edited by H. N. V. Temperly (North-Holland, Amsterdam, 1968), Chap. 5, p. 115.
- ¹⁸N. F. Carnahan and K. E. Starling, *J. Chem. Phys.* **51**, 635 (1969).
- ¹⁹J. M. Haile, C. Massobrio, and S. Torquato, *J. Chem. Phys.* **83**, 4075 (1985).
- ²⁰R. M. Ziff, *J. Chem. Phys.* (to be published).
- ²¹A. S. Sangani and C. Yao, *Phys. Fluids* **31**, 2426 (1988); **31**, 2435 (1988); P. P. Durand and L. H. Ungar, *Int. J. Num. Methods Eng.* **26**, 2487 (1988).
- ²²The large 490-particle systems used in all our simulations are especially necessary when the particles possess some degree of penetrability (i.e., for $\lambda < 1$), since in such instances the particles may overlap to form clusters. A particularly important state point occurs when an infinite cluster appears, i.e., at the percolation transition. Finite-size effects are known to be appreciable near and at criticality. See, for example, D. Stauffer, *Introduction to Percolation Theory* (Taylor and Francis, London, 1985).
- ²³M. Doi, *J. Phys. Soc. Jpn.* **40**, 567 (1976).
- ²⁴J. Rubinstein and S. Torquato, *J. Chem. Phys.* **88**, 6372 (1988); S. Torquato and J. Rubinstein, *ibid.* **90**, 1644 (1989).
- ²⁵Doi (Ref. 23) was the first to calculate the interfacial surface bound for fully penetrable spheres but did not tabulate his results.
- ²⁶P. M. Richards and S. Torquato, *J. Chem. Phys.* **87**, 4612 (1987).
- ²⁷R. I. Cukier and K. Freed, *J. Chem. Phys.* **78**, 2573 (1983); C. W. J. Beenakker and J. Ross, *ibid.* **84**, 3863 (1986).